



CHORUS

This is the accepted manuscript made available via CHORUS. The article has been published as:

Highly connected neurons spike less frequently in balanced networks

Ryan Pyle and Robert Rosenbaum

Phys. Rev. E **93**, 040302 — Published 27 April 2016

DOI: [10.1103/PhysRevE.93.040302](https://doi.org/10.1103/PhysRevE.93.040302)

Highly connected neurons spike less frequently in balanced networks

Ryan Pyle¹ and Robert Rosenbaum^{1,2}

¹*Department of Applied and Computational Mathematics and Statistics,
University of Notre Dame, Notre Dame IN 46556, USA*

²*Interdisciplinary Center for Network Science and Applications,
University of Notre Dame, Notre Dame IN 46556, USA*

Biological neuronal networks exhibit highly variable spiking activity. Balanced networks offer a parsimonious model of this variability in which strong excitatory synaptic inputs are canceled by strong inhibitory inputs on average and irregular spiking activity is driven by fluctuating synaptic currents. Most previous studies of balanced networks assume a homogeneous or distance-dependent connectivity structure, but connectivity in biological cortical networks is more intricate. We use a heterogeneous mean-field theory of balanced networks to show that heterogeneous in-degrees can break balance. Moreover, heterogeneous architectures that achieve balance promote lower firing rates in neurons with larger in-degrees, consistent with some recent experimental observations.

Many neuronal networks exhibit noisy and irregular activity [1–3], which is the focus of many theoretical studies [4–7], and also exhibit a balance between positive (excitatory) and negative (inhibitory) interactions [8–16]. Balanced network models offer a parsimonious model of this activity. In balanced networks, chaotic or chaos-like dynamics produce irregular spiking activity through transient fluctuations in the balance of strong excitatory and inhibitory currents [17–21]. Most studies of balanced networks assume a homogeneous network architecture where connection probability depends only on cell polarity. This was recently extended to networks with distant-dependent connection probabilities [22, 23], but biological networks exhibit more diverse architectures [24–27].

In this communication, we use mean-field theory to show that architectures with heterogeneous in-degree distributions and homogeneous out-degree distributions can break the classical balanced state, consistent with parallel studies [27–30]. We next show that balance can be restored, for example if out-degrees are also heterogeneous. In each of the example architectures we consider, neurons with higher in-degrees have lower firing rates, consistent with recent experimental results showing a negative correlation between firing rate and local functional coupling strength in cortex [31].

a. Model description. We consider a network of N integrate-and-fire neurons. The membrane potential of neuron j obeys

$$\frac{dV_j}{dt} = f(V_j) + I_j(t)$$

and each time $V_j(t)$ exceeds a threshold at V_{th} , the neuron spikes, the membrane potential is held for a refractory period τ_{ref} and then reset to V_{re} . All simulations use the exponential integrate-and-fire (EIF) model [39]. Synaptic input currents are defined by

$$I_j(t) = \sum_{k=1}^N \frac{J_{jk}}{\sqrt{N}} \sum_n \alpha_k(t - t_{k,n}) + \sqrt{N} F_j \quad (1)$$

where, $t_{k,n}$ is the n th spike time of neuron $k = 1, \dots, N$. Postsynaptic current waveforms satisfy $\alpha_k(t) = 0$ for $t < 0$ and $\int \alpha_k(t) dt = 1$ [40]. The term F_j models feed-forward input to the neuron from outside the network.

We are interested in the statistics of network activity as N grows large. The $N \times N$ connectivity matrix, J , is assumed random and our mean-field analysis only depends on the expected value of the entries of J .

b. Heterogeneous mean-field theory of balanced networks. We first extend the mean-field theory of firing rates in balanced networks [17–19, 23] to account for heterogeneous structure. We consider random networks partitioned into K populations and assume that the mean strength of synaptic connections between neurons in each pair of populations is known and $\mathcal{O}(1)$.

Specifically, assume that population m contains N_m neurons with $q_m = N_m/N \sim \mathcal{O}(1)$ for $m = 1, \dots, K$. The average input to neurons in population m is

$$\bar{I}_m = \text{avg}_{j \in G(m)} [I_j(t)]$$

where $j \in G(m)$ indicates that the average is taken over all neurons in population m , and also over time. Define \bar{F}_m similarly and define r_m to be the average spiking rate of neurons in population m . Averaging Eq. (1) over each population and over time gives the mean-field mapping

$$\vec{I} = \sqrt{N} (W\vec{r} + \vec{F}) \quad (2)$$

where $\vec{I} = [\bar{I}_1 \dots \bar{I}_K]$ is the vector of mean inputs and similarly for \vec{r} and \vec{F} . The $K \times K$ mean-field connectivity matrix is defined by

$$W = [q_n \bar{J}_{mn}]_{m,n=1}^K$$

where

$$\bar{J}_{mn} = \frac{1}{N_m N_n} \sum_{j \in G(m), k \in G(n)} J_{jk}$$

is the mean connection strength from neurons in population n to those in population m , assumed to be $\mathcal{O}(1)$.

In the balanced state, $\vec{r}, \vec{I} \sim \mathcal{O}(1)$ as N increases. From Eq. (2), however, this can only be achieved under a cancellation between positive and negative (excitatory and inhibitory) input sources in such a way that $W\vec{r} + \vec{F} \sim \mathcal{O}(1/\sqrt{N})$. This cancellation defines the balanced network state [17, 18]. As $N \rightarrow \infty$, firing rates are given by the solution to the balance equation

$$W\vec{r} + \vec{F} = 0. \quad (3)$$

Thus, the existence of a balanced state requires that Eq. (3) has a solution, \vec{r} , with positive components, $r_m > 0$. When W is invertible, this solution can be written as $\lim_{N \rightarrow \infty} \vec{r} = -W^{-1}\vec{F}$.

The mean-field analysis above only considers the existence of a balanced fixed point, but this fixed point must be stable for balance to be realized. When membrane and synaptic dynamics are mostly homogeneous in the network, stability can be approximated by considering the dynamical mean-field equation [23, 32, 33]

$$\tau_m \vec{r}' = -\vec{r} + f\left(\sqrt{N}[W\vec{r} + \vec{F}]\right) \quad (4)$$

where $f(\cdot)$ is a non-decreasing firing rate function and τ_m is the neurons' membrane time constant. For integrate-and-fire models, we can assume that f is a threshold-linear function and conclude that stability is achieved for large N when all eigenvalues of W have negative real part [23]. A more precise stability analysis uses a diffusion approximation and accounts for synaptic kinetics [19, 34, 35], but the simpler approach here has been successfully applied to balanced networks [18, 23].

c. A review of homogeneous balanced networks. For the purpose of comparison, we first review networks with homogeneous connection probabilities that depend only on cell polarity (excitatory or inhibitory) as in [17, 18]. For this model, $N_e = q_e N$ of the neurons are excitatory and $N_i = q_i N$ are inhibitory, where $q_e, q_i \sim \mathcal{O}(1)$. All excitatory neurons receive the same feedforward input, $F_j = F_e > 0$, and all inhibitory neurons receive $F_j = F_i > 0$. The synaptic connection strength, J_{jk} , from neuron k in population $y = e, i$ to neuron j in population $x = e, i$ are randomly assigned according to

$$J_{jk} = \begin{cases} j_{xy} & \text{with prob. } p_{xy} \\ 0 & \text{otherwise} \end{cases}.$$

Here, p_{xy} represents the connection probability from population $y = e, i$ to population $x = e, i$ and j_{xy} represents the strength of each such connection. Note that $j_{ee}, j_{ie} > 0$ and $j_{ei}, j_{ii} < 0$.

Dividing the network into excitatory and inhibitory populations and applying the mean-field theory outlined above gives the mean feedforward input, $\vec{F} = [F_e \ F_i]^T$ and mean-field connectivity matrix

$$W_h = \begin{bmatrix} w_{ee} & w_{ei} \\ w_{ie} & w_{ii} \end{bmatrix} \quad (5)$$

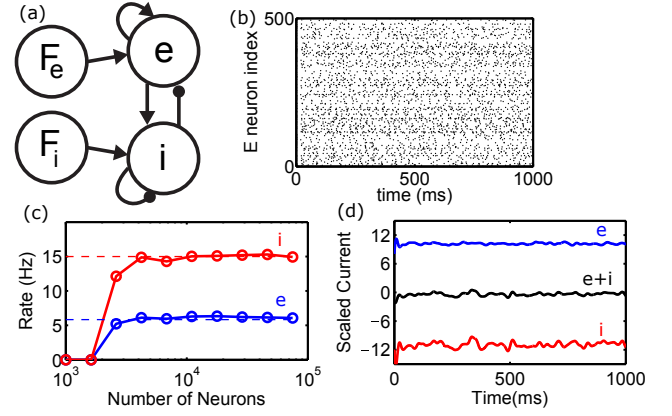


FIG. 1: **A homogeneous balanced network.** (a) Network schematic. A population of N_e excitatory and N_i inhibitory neurons (e and i) are randomly connected and also receive feedforward input (F_e and F_i). (b) Raster of plot of 500 randomly sampled excitatory neurons from a simulation of a balanced network with $N_e = 4 \times 10^4$ and $N_i = 10^4$. (c) Firing rates from simulations (solid curves) approach the values predicted by solving Eq. (3) (dashed lines) as network size, $N = N_e + N_i$, grows. (d) Synaptic input to one representative excitatory neuron shows that strong excitatory currents (blue) balance with strong inhibitory currents (red) to yield a moderate total synaptic current (black). Synaptic currents were convolved with a Gaussian shaped filter ($\sigma = 8$ ms) and normalized by the neuron's rheobase.

where $w_{xy} = q_y p_{xy} j_{xy}$ and the subscript h , for homogeneous, is used to distinguish this matrix from the ones we will consider below. For this network, the balance equation (3) has a stable, positive solution whenever [17–19, 23]

$$\frac{F_e}{F_i} > \frac{w_{ei}}{w_{ii}} > \frac{w_{ee}}{w_{ie}}. \quad (6)$$

Computer simulations [41] confirm the predicted firing rates and demonstrate the asynchronous, irregular spiking characteristic of the balanced state (Fig. 1). We next show that re-wiring this network to produce heterogeneous in-degrees can break balance.

d. Heterogeneous in-degrees can break balance. As a first example of a heterogeneous network, we re-wired the homogeneous network above to produce a bimodal distribution of in-degrees. We first partitioned the excitatory population into two equal-sized sub-populations, e_1 and e_2 . We then did the same for the inhibitory population, giving a total of $K = 4$ sub-populations which we enumerate as e_1, i_1, e_2 and i_2 .

A proportion $c_{in} = 1/5$ of the incoming connections to postsynaptic neurons in populations e_1 and i_1 were randomly re-assigned to postsynaptic neurons in populations e_2 and i_2 respectively. Thus, the average in-degrees of neurons in populations e_2 and i_2 were larger than those of neurons in populations e_1 and i_1 respectively (Fig. 2a). The out-degrees and feedforward inputs were unchanged from Fig. 1.

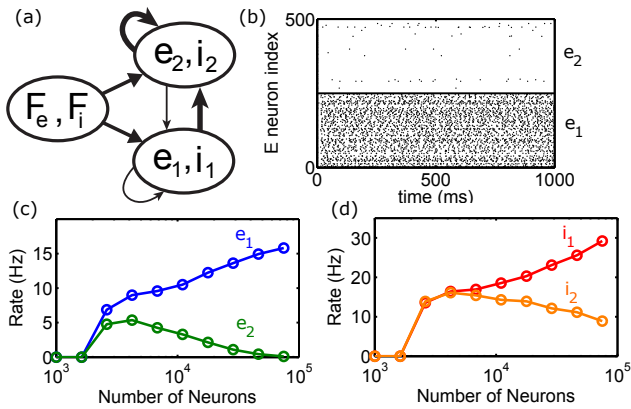


FIG. 2: **Heterogeneous in-degrees can break balance.** (a) Network diagram. Same as network in Fig. 1 except excitatory and inhibitory populations were each split into two populations. Neurons in populations e_2 and i_2 have larger in-degrees than those in e_1 and i_1 . (b) Raster plot of 500 randomly selected excitatory neurons, half from e_1 and half from e_2 , from a simulation with $N = 5 \times 10^4$ neurons. (c,d) Mean firing rate in each population as a function of network size (N).

In simulations of this network, the average firing rates of neurons in populations e_1 and i_1 were larger than the excitatory and inhibitory rates in populations e_2 and i_2 (Fig. 2b-d). Thus, perhaps surprisingly, a higher in-degree was associated with lower firing rates. Increasing the network size while keeping connection probability fixed exaggerated this effect as firing rates in population e_2 approached zero (Fig. 2c,d).

To understand this phenomenon intuitively, consider a simplified network diagram in which the populations with decreased in-degrees (e_1 and i_1) are grouped together (group 1) and those with increased in-degrees (e_2 and i_2) are also grouped together (group 2, Fig. 2a). The increased in-degree of group 2 is then the equivalent of an increase in the mean strength of its self-connections and the mean strength of group-2-to-group-1 connections (indicated by thicker arrows in Fig. 2a).

In the balanced state, strong inhibition cancels strong excitation, including excitatory feedforward input. While both groups receive identical feedforward input, group 2 receives more recurrent input than group 1 regardless of the firing rates of each population. Balance cannot be maintained in both groups because the same level of feedforward input received by each group cannot be simultaneously balanced by the two different levels of recurrent input they receive. Group 2 receives an excess of inhibition because recurrent connections are net inhibitory in balanced networks [17, 18], explaining why group 2 has lower firing rates than group 1.

A more rigorous understanding is provided by applying the heterogeneous mean-field analysis described above. The 4×1 vector of mean feedforward inputs to populations e_1, i_1, e_2 and i_2 is given by $\vec{F} = [F_e \ F_i \ F_e \ F_i]^T$. The 4×4 mean-field connectivity matrix is given in

block form by

$$W = \frac{1}{2} \begin{bmatrix} (1 - c_{in})W_h & (1 - c_{in})W_h \\ (1 + c_{in})W_h & (1 + c_{in})W_h \end{bmatrix}$$

where W_h is the 2×2 matrix from Eq. (5).

Note that W is singular and its range does not contain \vec{F} . Thus, Eq. (3) does not admit a solution and this network re-wiring destroys balance. As a result, firing rates in group 2 approach zero as $N \rightarrow \infty$ due to an excess of recurrent inhibition. Thus, re-wiring a homogeneous network to achieve heterogeneous out-degrees can destroy balance [27–30], causing highly connected sub-populations to cease spiking.

This loss of balance was caused by the singularity of W , which is a null-property of matrices since the perturbed matrix $W + \epsilon A$ is almost surely invertible for random matrices, A , with entries drawn independently from an absolutely continuous distribution. However, the perturbed firing rate vector, given by $\vec{r} = -(W + \epsilon A)^{-1}\vec{F}$, is almost surely $\mathcal{O}(1/\epsilon)$. Thus, connectivity structures that are inconsistent with balance promote large firing rates even when they are only approximately realized. Moreover, balance requires that the firing rate solutions are positive, so not all perturbations of a singular W give a balanced solution. Nevertheless, there are numerous modifications of the network that can recover balance. We next consider some examples.

e. Recovering balance promotes lower firing rates in neurons with more synaptic inputs. The re-wiring of the homogeneous network considered above only altered in-degrees of neurons. Starting from this rewiring, we now also change the out-degrees by rewiring the source of some edges. Specifically, a proportion $c_{out} = 4/5$ of the synaptic projections from presynaptic neurons in population e_1 to postsynaptic neurons in population e_2 are rewired to emanate from randomly selected presynaptic neurons in population e_2 , *i.e.* they now project from e_2 to e_2 . Similarly, a proportion $c_{out} = 4/5$ of projections from neurons in x_1 to neurons in y_2 are rewired to form x_2 -to- y_2 projections for all pairings of $x, y \in \{e, i\}$.

This rewiring increases the average out-degree of neurons in populations e_2 and i_2 by a proportion c_{out} and decreases the out-degrees of neurons in population e_1 and i_1 by the same proportion. Since e_2 and i_2 also have larger in-degrees, this results in positively correlated in- and out-degrees (Fig. 3a).

Simulating this network, we found that the average firing rates of neurons in populations e_1 and i_1 were larger than the rates in populations e_2 and i_2 respectively (Fig. 3b-d), but the difference was less drastic than the example with just heterogeneous in-degrees (compare to Fig. 2). Increasing the network size while keeping connection probability fixed caused rates to approach non-zero limits (Fig. 3c,d).

Repeating the mean-field analysis from above, the 4×4 mean-field connectivity matrix is given in block form

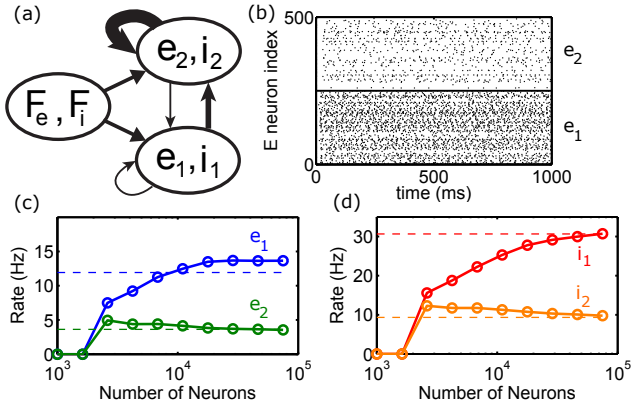


FIG. 3: **Balance can be restored by heterogeneous out-degrees.** Same as Fig. 2, except out-degrees of neurons in populations e_2 and i_2 were increased by rewiring a proportion $c_{\text{out}} = 4/5$ of the outgoing projections from populations e_1 and i_1 to project from e_2 and i_2 instead. Dashed lines shows the asymptotic firing rates predicted by Eq. (3).

by

$$W = \frac{1}{2} \begin{bmatrix} (1 - c_{\text{in}})W_h & (1 - c_{\text{in}})W_h \\ (1 + c_{\text{in}})(1 - c_{\text{out}})W_h & (1 + c_{\text{in}})(1 + c_{\text{out}})W_h \end{bmatrix}$$

where W_h is from Eq. (5). For this example, the network admits a stable balanced state, *i.e.* Eq. (3) has positive solutions and the eigenvalues of W are negative. As predicted, the balanced firing rates given by $\vec{r} = -W^{-1}\vec{F}$ agree with network simulations for large N (Fig. 3c,d). Interestingly, neurons with larger in-degrees (those in populations e_2 and i_2) have lower firing rates. We next show that this is a prevailing feature of heterogeneous balanced networks.

We have so far considered heterogeneous networks constructed by breaking a homogeneous balanced network into $K = 4$ populations (two excitatory and two inhibitory), then modifying the connection probability between each of the four populations. Generalizing this approach, we can consider multiplying the connection probability from populations e_k and i_k to populations e_j and i_j by some factor a_{jk} for $j, k = 1, 2$. This gives a mean-field connectivity matrix of the form

$$W = \begin{bmatrix} a_{11}W_h & a_{12}W_h \\ a_{21}W_h & a_{22}W_h \end{bmatrix}.$$

As before, we leave the feedforward inputs unchanged, $\vec{F} = [F_e \ F_i \ F_e \ F_i]^T$.

See Supplemental Material at [URL will be inserted by publisher] for a proof that this network admits a stable balanced state only if populations project to themselves with a higher probability than they project to each other ($a_{11} > a_{21}$ and $a_{22} > a_{12}$) and that, under this condition, populations with higher in-degree have lower firing rates.

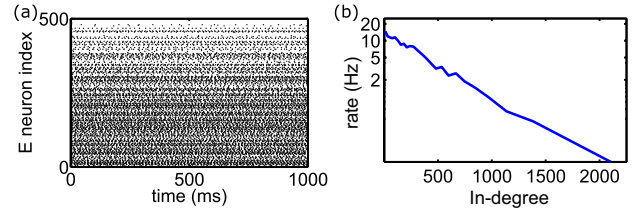


FIG. 4: **Dependence of firing rates on in-degree in a scale free network.** (a) Raster plot and (b) firing rates as a function of in-degree from a network of 5×10^4 neurons with a power-law distribution of in-degrees. For the raster plot, 500 excitatory neurons were sampled uniformly from the network and sorted so that in-degree increased with “neuron index.”

Note that it is still possible to construct a balanced network with two excitatory and two inhibitory populations such that populations with larger in-degree have larger rates. For example, one could increase the feedforward input to neurons with larger in-degree. However, our results suggest that balance promotes lower firing rates in neurons with more inputs. This can be explained intuitively by noting that recurrent input is net-inhibitory in balanced networks, so neurons with more local inputs tend to receive more inhibition.

So far, we have focused on networks with two excitatory and two inhibitory population. See Supplemental Material at [URL will be inserted by publisher] for numerical examples demonstrating that the negative correlation between in-degree and firing rates persists when a larger number of populations is considered.

In conclusion, networks with discrete populations can achieve balance, but balance promotes lower firing rates in neurons with higher in-degrees because recurrent connections are net-inhibitory in balanced networks. We next investigate whether this finding carries over to a continuously indexed network.

f. Firing rates in a scale free network. We assign to each neuron an in-degree, u , drawn independently from a generalized Pareto distribution with density function

$$Q(u) = \begin{cases} \frac{1}{\sigma} \left(1 + \frac{u-\mu}{\sigma}\xi\right)^{-(\xi^{-1}-1)} & u \geq \mu \\ 0 & u < \mu \end{cases}$$

with shape parameter $\xi = 0.25$, location parameter $\mu = 5$ and scale parameter, $\sigma = (\bar{p}N - \mu)(1 - \xi)$, giving an average connection probability, $\bar{p} = 0.05$. We then draw $\text{round}(u)$ excitatory and inhibitory presynaptic neurons randomly and uniformly from the network. Thus, in-degrees obey a power-law distribution, but out-degrees are approximately homogeneous. Feedforward input strengths depend only on cell polarity, as above.

Simulating this network confirms that firing rates are lower for neurons with higher in-degree (Fig. 4), analogous to the networks considered above.

The heterogeneous mean-field analysis outlined above can be applied by partitioning the network according to in-degree and neuron polarity. In the limit

of large N and finer partitions, the matrix equation (3) is approximated by a system of integral equations (compare to spatial networks in [23]),

$$\begin{aligned} \int_{\mu}^{\infty} [w_{ee}(u, v)r_e(v) - w_{ei}(u, v)r_i(v)]dv + F_e &= 0 \\ \int_{\mu}^{\infty} [w_{ie}(u, v)r_e(v) - w_{ii}(u, v)r_i(v)]dv + F_i &= 0. \end{aligned} \quad (7)$$

Here, $r_x(v)$ is the average firing rate of neurons in population $x = e, i$ with in-degree v . The term

$$w_{xy}(u, v) = Q(v)j_{xy}p(u, v)$$

represents mean-field connectivity from neurons in population $y = e, i$ with in-degree v to neurons in population $x = e, i$ with in-degree u where $p(u, v)$ represents the probability and j_{xy} the strength of such a connection. For the example considered here, connection probability depends only on the in-degree of the post-synaptic neuron so that $p(u, v) = u/N$. Note that $u \sim \mathcal{O}(N)$ so that $p(u, v) \sim \mathcal{O}(1)$ on average. Thus Eqs. (7) become

$$\frac{u}{N} [j_{xe}\bar{r}_e - j_{xi}\bar{r}_i] + F_x = 0, \quad x = e, i$$

where $\bar{r}_x = \int Q(v)r_x(v)dv$ is the average firing rate of neurons in population $x = e, i$. For balance to be achieved, this equation must be satisfied simultaneously for all $u > \mu$, which is not possible. We conclude that the network in Fig. 4 violates the balanced state.

Restoring balance in this example would require building a family of networks indexed by N , where connection probability, $p(u, v) \sim \mathcal{O}(1)$, depends on pre- and post-synaptic in-degree, u and v , in such a way that Eqs. (7) are solvable with $r_x(v) \geq 0$. Balance could also be restored by allowing feedforward input to depend on in-degree, $F_x \rightarrow F_x(u)$, in such a way that Eqs. (7) are solvable. However, unlike the matrix equation (3), the system of integral equations in (7) are not generically solvable. Specifically, since Eq. (7) is an integral equation of the first kind, for any connectivity kernels, $w_{xy}(u, v)$, there are feedforward inputs, $F_x(u)$, such that Eq. (7) does not admit a solution [36].

g. Discussion. We used mean-field theory to analyze structured balanced networks. Similar to the theory of homogeneous and spatially-extended balanced networks, firing rates in the limit of large network size are

determined by a linear equation [17–19, 23]. The solvability of this equation determines the existence of the balanced state in the thermodynamic limit.

We found that balance is promoted by architectures where populations connect to themselves more strongly than they connect to each other. Moreover, we showed that balance promotes lower firing rates in neurons with a larger number of inputs from the local network. This is explained by the fact that recurrent input is net-inhibitory in balanced networks [17–19]. This observation could explain the negative correlation between firing rate and local population coupling recently observed in cortical recordings [31].

Our mean field analysis only relied on the assumption that synaptic integration is linear and that firing rates are $\mathcal{O}(1)$ as N increases. Thus, our findings are applicable to neuron models with more detailed membrane dynamics, like the Fitzhugh-Nagumo model.

The imbalance created by heterogeneous in-degrees suppresses spiking in some neurons and increases rates in others as $N \rightarrow \infty$ (Fig. 2). Biological networks are, of course, finite in size. At sufficiently small N , rates can be positive even if Eq. (3) has no positive solution (as in Fig. 2c,d). Firing rates in such finite sized networks could potentially be approximated numerically using a diffusion approximation that yields a system of non-linear fixed point equations [19, 34].

A parallel study reached the same conclusion that balance can be broken by heterogeneous in-degrees, but recovered balance through an adaptation current [27–29]. This resolution requires that adaptation currents are $\mathcal{O}(\sqrt{N})$ to cancel excess synaptic input. This could be reasonable at the finite sizes of biological networks.

Previous studies consider recurrent neuronal networks with various types of heterogeneous connectivity structures [37, 38], but not in the balanced state. Future work will consider the application of our balanced mean-field theory to these alternative architectures.

I. ACKNOWLEDGMENTS

This work was supported by NSF-DMS-1517828.

[1] W. R. Softky and C. Koch, *J Neurosci* **13**, 334 (1993).
 [2] M. N. Shadlen and W. T. Newsome, *Curr Op Neurobiol* **4**, 569 (1994).
 [3] A. A. Faisal, L. P. Selen, and D. M. Wolpert, *Nat Rev Neurosci* **9**, 292 (2008).
 [4] D. Valenti, G. Augello, and B. Spagnolo, *Eur Phys J B* **65**, 443 (2008).
 [5] Y. V. Ushakov, A. A. Dubkov, and B. Spagnolo, *Phys Rev*

E **81**, 041911 (2010).
 [6] Y. V. Ushakov, A. Dubkov, and B. Spagnolo, *Phys Rev Lett* **107**, 108103 (2011).
 [7] W. Gerstner, W. M. Kistler, R. Naud, and L. Paninski, *Neuronal dynamics: From single neurons to networks and models of cognition* (Cambridge University Press, Cambridge, 2014).
 [8] Y. Shu, A. Hasenstaub, and D. A. McCormick, *Nature*

- 423, 288 (2003).
- [9] M. Wehr and A. M. Zador, *Nature* **426**, 442 (2003).
- [10] J. Mariño, J. Schummers, D. C. Lyon, L. Schwabe, O. Beck, P. Wiesing, K. Obermayer, and M. Sur, *Nat Neurosci.* **8**, 194 (2005).
- [11] B. Haider, A. Duque, A. R. Hasenstaub, and D. A. McCormick, *J Neurosci* **26**, 4535 (2006).
- [12] M. Okun and I. Lampl, *Nat Neurosci* **11**, 535 (2008).
- [13] A. L. Dorrn, K. Yuan, A. J. Barker, C. E. Schreiner, and R. C. Froemke, *Nature* **465**, 932 (2010).
- [14] Y. J. Sun, G. K. Wu, B.-h. Liu, P. Li, M. Zhou, Z. Xiao, H. W. Tao, and L. I. Zhang, *Nature* **465**, 927 (2010).
- [15] M. Zhou, F. Liang, X. R. Xiong, L. Li, H. Li, Z. Xiao, H. W. Tao, and L. I. Zhang, *Nat Neurosci* **17**, 841 (2014).
- [16] P. C. Petersen, M. Vestergaard, K. H. R. Jensen, and R. W. Berg, *J Neurosci* **34**, 2774 (2014).
- [17] C. van Vreeswijk and H. Sompolinsky, *Science* **274**, 1724 (1996).
- [18] C. van Vreeswijk and H. Sompolinsky, *Neural Comput* **10**, 1321 (1998).
- [19] A. Renart, N. Brunel, and X.-J. Wang, in *Computational Neuroscience: A Comprehensive Approach* (CRC Press, Boca Raton, 2004) pp. 431–490.
- [20] M. Monteforte and F. Wolf, *Phys Rev X* **2**, 041007 (2012).
- [21] G. Lajoie, K. K. Lin, and E. Shea-Brown, *Phys. Rev. E* **87**, 052901 (2013).
- [22] S. Lim and M. S. Goldman, *Nat Neurosci* **16**, 1306 (2013).
- [23] R. Rosenbaum and B. Doiron, *Phys Rev X* **4**, 021039 (2014).
- [24] S. Song, P. J. Sjöström, M. Reigl, S. Nelson, and D. B. Chklovskii, *PLoS Biol* **3**, e68 (2005).
- [25] a. J. Sadvovsky and J. N. MacLean, *J. Neurosci.* **33**, 14048 (2013).
- [26] S. S. Gururangan, A. J. Sadvovsky, and J. N. MacLean, *PLoS Comput. Biol.* **10**, e1003710 (2014).
- [27] I. Landau, R. Egger, M. Oberlaender, and H. Sompolinsky, “The relationship between microcircuit structure and dynamics in the rat barrel cortex,” Society for Neuroscience Meeting 2014, Washington, D.C., USA (2014).
- [28] I. Landau, R. Egger, V. Dercksen, M. Oberlaender, and S. H., “Slow adaptation facilitates excitation-inhibition balance in the presence of structural heterogeneity,” Cosyne Abstracts 2016, Salt Lake City, USA (2016).
- [29] I. Landau and S. H., “Realistic structural heterogeneity in local circuits and its implications on the balanced state.” Cosyne Abstracts 2015, Salt Lake City, USA (2015).
- [30] M. Veué and A. Roxin, “Different models of network connectivity can explain non-random features of cortical microcircuits,” Society for Neuroscience Meeting 2015, Chicago, Illinois, USA (2015).
- [31] M. Okun, N. a. Steinmetz, L. Cossell, M. F. Iacaruso, H. Ko, P. Barthó, T. Moore, S. B. Hofer, T. D. Mrsic-Flogel, M. Carandini, and K. D. Harris, *Nature* **521**, 511 (2015).
- [32] P. Dayan and L. F. Abbott, *Theoretical Neuroscience* (MIT Press, MA, 2001).
- [33] G. B. Ermentrout and D. H. Terman, *Mathematical foundations of neuroscience* (Springer Science & Business Media, New York, 2010).
- [34] D. Amit and N. Brunel, *Cereb Cortex* **7**, 237 (1997).
- [35] E. Ledoux and N. Brunel, *Front Comput Neurosci* **5**, 25 (2011).
- [36] F. G. Tricomi, *Integral equations* (Interscience, New York, 1957).
- [37] L. Zhao, I. Bryce Beverlin, T. Netoff, and D. Q. Nykamp, *Front Comp Neurosci* **5**, 1 (2011).
- [38] J. M. Beggs and D. Plenz, *J Neurosci* **23**, 11167 (2003).
- [39] EIF model defined by defined by $\tau_m f(V) = -(V - E_L) + \Delta_T \exp[(V - V_T)/\Delta_T]$ with parameters $\tau_m = 15\text{ms}$, $\Delta_T = 2\text{ mV}$, $V_T = -55\text{ mV}$, $V_{th} = -50\text{ mV}$, $V_{re} = -75\text{ mV}$ and $\tau_{ref} = 0.5\text{ ms}$
- [40] For all simulations, $\alpha_k(t) = (e^{-t/\tau_d} - e^{-t/\tau_r})/(\tau_d - \tau_r)$ for $t > 0$ with timescales $\tau_d = 0.1$ and $\tau_r = 6$ for excitatory presynaptic neurons and $\tau_d = 0.1$ and $\tau_r = 4$ for inhibitory neurons.
- [41] Parameters for all simulations: $j_{ee} = 112.5$, $j_{ei} = -300$, $j_{ie} = 225$, $j_{ii} = -450$, $F_e = 0.0187$, $F_i = 0.015$, $q_e = 0.8$, $q_i = 0.2$ and $p_{xy} = 0.05$ for $x, y \in \{e, i\}$.